Optical properties of random alloys: application to CuAu and NiPt

2005 J. Phys.: Condens. Matter 17 4559

(http://iopscience.iop.org/0953-8984/17/28/014)

INSTITUTE OF PHYSICS PUBLISHING JOURNAL OF PHYSICS: CONDENSED MATTER

J. Phys.: Condens. Matter **17** (2005) 4559–4566 doi:10.1088/0953-8984/17/28/014

Optical properties of random alloys: application to CuAu and NiPt

Kamal Krishna Saha and Abhijit Mookerjee

S N Bose National Centre for Basic Sciences, Block-JD, Sector-III, Salt Lake City, Kolkata-700098, India

Received 30 May 2005
Published 1 July 2005
Online at stacks.iop.org/JPhysCM/17/4559

Abstract

In an earlier paper we presented a formulation for the calculation of the configuration-averaged optical conductivity in random alloys. Our formulation is based on the augmented-space theorem introduced by one of us (Mookerjee 1973 *J. Phys. C: Solid State Phys.* **6** 1340). In this communication we shall combine the augmented space methodology with the tight-binding linear muffin-tin orbital technique (TB-LMTO) to study the optical conductivities of two alloys, CuAu and NiPt.

(Some figures in this article are in colour only in the electronic version)

1. Introduction

In an earlier communication [1] we developed a formalism for the calculation of the configuration-averaged optical conductivity of a disordered binary alloy. We showed that the dominant effect of disorder is to renormalize each propagator as well as the current term in the Kubo formula. Other corrections involve joint fluctuation of two currents and a propagator and the vertex corrections in the ladder approximation. In this communication we propose to study the optical properties of disordered CuAu and NiPt alloys from this first principles approach. We have chosen these two alloy systems for several reasons: for CuAu, the bunch of d-like states sits about 2 eV below the Fermi level. For low photon energies, therefore, optical conductivity is dominated by the intra-band transitions within s–p-like states, which are extended and rather free-electron-like. As a consequence, the optical conductivity for low photon energies below $\simeq$2 eV should have a Drude-like behaviour. For higher photon energies inter-band transitions between the occupied d states and the higher unoccupied states begin to take over. In sharp contrast, the Fermi energy of NiPt almost straddles the d-like peak. For this alloy the Drude behaviour should be confined to a very narrow low photon energy range. This contrasting behaviour should be reflected in our results.

Earlier theoretical work on optical conductivity for random alloys began with Velický [2], based on the single-site coherent potential approximation (CPA) in an empirical tight-binding model alloy. Butler [3] extended the ideas and combined the CPA with the first principles

Korringa–Kohn–Rostoker (KKR) technique. Development of the KKR-CPA should also include the work of Gyorffy and Stott [4], Gyorffy and Stocks [5] and Gyorffy and Winter [6]. Scott and Muldawer [7] have obtained high resolution optical data for ordered and disordered CuAu alloys for polycrystalline films for photon energies between 1.2 and 6.2 eV. We shall compare our theoretical results with theirs. Banhart [8] used the KKR-CPA to study the optical conductivity of AgAu alloys. This alloy system has a close resemblance to CuAu. Banhart found discrepancies of his theoretical results with experiment [10, 11] and argued that various factors could be responsible: first, the use of the density functional and the single-site mean-field approximations in theory. The augmented space recursion (ASR) technique proposed by us [12] goes beyond the single-site mean-field approximation and includes fluctuations without violating Herglotz analyticity of the configuration-averaged Green functions. The suitability of the ASR for the study of disordered alloys has been discussed in a series of papers by us and we direct the reader's attention to them [13]. Moreover, in both the alloy systems there is a large size mismatch between the constituents. In an earlier paper [14] we discussed in detail how to deal with local lattice distortions due to size mismatch between the constituents of an alloy within the ASR. We applied it to two alloy systems, CuPd and CuBe, and the reader is referred to the paper for details. Second, there are also effects of surfaces, their roughness, possible adsorbates and presence of large stresses in the samples, in the experiments. Gunnarsson *et al* [9] report theoretical calculations of $\sigma(\omega)$ for Nb_3Sb, which is similar to NiPt, in the sense that in both alloys the Fermi level sits right on the d-like peaks and we expect Drude-like behaviour only in a very narrow range of photon energies. Again, we shall compare our results with them. There have been a few more theoretical studies of optical properties of random alloys: Rhee *et al* [15] on CoAl, Uba *et al* [16] on CoPt and Rhee *et al* [17] on Ni_3Al. These works all base their approach on a large super-cell method to take care of the disorder.

In our earlier paper [1], substitutional disorder dictated our choice of a purely real-space representation and we had chosen as our basis the minimal set of the tight-binding linear muffin-tin orbital (TB-LMTO) method [18, 19]. Configuration averaging over various random atomic arrangements had been carried out using the augmented-space formalism (ASF) introduced by us earlier for the study of electronic properties of disordered systems [13, 14, 20, 21]. As mentioned earlier, the ASF goes beyond the usual single-site mean-field approaches and takes into account configuration fluctuations about the mean field. We shall present here a summary of the results derived in the earlier paper [1]. In linear response theory, at zero temperature, the real part of the optical conductivity of a disordered alloy is given by the Kubo–Greenwood expression [22]:

$$\sigma(\omega) = \frac{S(\omega)}{\omega} \tag{1}$$

where the configuration-averaged current–current correlation function $\langle\langle S(\omega)\rangle\rangle$ is given by

$$\frac{1}{3\pi}\sum_{\gamma}\mathrm{Tr}\int \mathrm{d}E\,\langle \mathbf{j}_\gamma\,\mathrm{Im}\{\mathbf{G}^{v}(E)\}\mathbf{j}_\gamma^{\dagger}\,\mathrm{Im}\{\mathbf{G}^{c}(E+\omega)\}\rangle. \tag{2}$$

If we define

$$\langle\langle S_\gamma(z_1, z_2)\rangle\rangle = \mathrm{Tr}\langle \mathbf{j}_\gamma \mathbf{G}^{v}(z_1)\mathbf{j}_\gamma^{\dagger}\mathbf{G}^{c}(z_2)\rangle, \tag{3}$$

then, using the Herglotz[1] properties of the Green function, the correlation function becomes

$$\begin{aligned}\langle\langle S(\omega)\rangle\rangle = \frac{1}{12\pi}\sum_{\gamma}\int \mathrm{d}E\,[&\mathcal{S}_\gamma(E^-, E^+ + \omega) + \mathcal{S}_\gamma(E^+, E^- + \omega)\ldots \\ &- \mathcal{S}_\gamma(E^+, E^+ + \omega) - \mathcal{S}_\gamma(E^-, E^- + \omega)]\end{aligned} \tag{4}$$

[1] A function $f(z)$ of a complex variable z is called *Herglotz* if (i) all the singularities lie on the real axis, (ii) $\mathrm{sgn}(\mathrm{Im}\, f(z)) = -\mathrm{sgn}(\mathrm{Im}\, z)$ and (iii) $f(x) \to 0$, $z = x + \mathrm{i}0$ and $x \to \pm\infty$.

where

$$F(E^{\pm}) = \lim_{\delta \to 0} F(E \pm \mathrm{i}\delta).$$

It was shown in our earlier paper that one of the dominant contributions to the configuration-averaged correlation function was due to joint fluctuations of one current and a propagator:

$$\langle\!\langle S_{\gamma}^{(1)}(z_1, z_2)\rangle\!\rangle = \int_{\mathrm{BZ}} \frac{\mathrm{d}^3\mathbf{k}}{8\pi^3} \operatorname{Tr}[\mathbf{J}_{\gamma}^{\mathrm{eff}}(\mathbf{k}, z_1, z_2)\langle\!\langle \mathbf{G}^{v}(\mathbf{k}, z_1)\rangle\!\rangle \mathbf{J}_{\gamma}^{\mathrm{eff}}(\mathbf{k}, z_1, z_2)^{\dagger}\langle\!\langle \mathbf{G}^{c}(\mathbf{k}, z_2)\rangle\!\rangle] \tag{5}$$

where the effective current was

$$\begin{aligned}\mathbf{J}_{\gamma}^{\mathrm{eff}}(\mathbf{k}, z_1, z_2) = {} & \langle\!\langle \mathbf{j}_{\gamma}(\mathbf{k})\rangle\!\rangle + 2[\boldsymbol{\Sigma}(\mathbf{k}, z_2)\mathbf{f}(z_2)\mathbf{j}_{\gamma}^{(1)}(\mathbf{k}) + \mathbf{j}_{\gamma}^{(1)}(\mathbf{k})\mathbf{f}(z_1)\boldsymbol{\Sigma}(\mathbf{k}, z_1)] \ldots \\ & + \boldsymbol{\Sigma}(\mathbf{k}, z_2)\mathbf{f}(z_2)\mathbf{j}_{\gamma}^{(2)}(\mathbf{k})\mathbf{f}(z_1)\boldsymbol{\Sigma}(\mathbf{k}, z_1).\end{aligned} \tag{6}$$

The contribution of joint fluctuations between the two current terms and one propagator was given by

$$\begin{aligned}\langle\!\langle S_{\gamma}^{(2)}(z_1, z_2)\rangle\!\rangle = {} & 4\int_{\mathrm{BZ}} \frac{\mathrm{d}^3\mathbf{k}}{8\pi^3} \operatorname{Tr}[\mathbf{j}_{\gamma}^{(1)}(\mathbf{k})\mathbf{f}(z_1)\boldsymbol{\Sigma}(\mathbf{k}, z_1)\mathbf{f}(z_1)\mathbf{j}_{\gamma}^{(1)}(\mathbf{k})^{\dagger}\langle\!\langle \mathbf{G}(\mathbf{k}, z_2)\rangle\!\rangle \ldots \\ & + \mathbf{j}_{\gamma}^{(1)}(\mathbf{k})^{\dagger}\mathbf{f}(z_2)\boldsymbol{\Sigma}(\mathbf{k}, z_2)\mathbf{f}(z_2)\mathbf{j}_{\gamma}^{(1)}(\mathbf{k})\langle\!\langle \mathbf{G}(\mathbf{k}, z_1)\rangle\!\rangle].\end{aligned} \tag{7}$$

The vertex correction terms in the ladder approximation contributed

$$\begin{aligned}\langle\!\langle S_{\gamma}^{\mathrm{ladder}}(z_1, z_2)\rangle\!\rangle &= \operatorname{Tr} \sum_{L_1L_2} \sum_{L_3L_4} \Gamma_{\gamma}^{L_1L_2}(z_1, z_2)\Lambda_{L_2L_4}^{L_1L_3}\hat{\Gamma}_{\gamma}^{L_3L_4}(z_1, z_2) \\ &= \operatorname{Tr} \boldsymbol{\Gamma}_{\gamma}(z_1, z_2) \otimes \hat{\boldsymbol{\Gamma}}_{\gamma}(z_1, z_2)\Lambda(z_1, z_2)\end{aligned} \tag{8}$$

where

$$\int_{\mathrm{BZ}} \frac{\mathrm{d}^3\mathbf{k}}{8\pi^3} \mathbf{G}(\mathbf{k}, z_2)\mathbf{J}_{\gamma}^{\mathrm{eff}}(\mathbf{k}, z_1, z_2)\mathbf{G}(\mathbf{k}, z_1) = \boldsymbol{\Gamma}_{\gamma}(z_1, z_2)$$

$$\int_{\mathrm{BZ}} \frac{\mathrm{d}^3\mathbf{k}'}{8\pi^3} \mathbf{G}(\mathbf{k}', z_1)\mathbf{J}_{\gamma}^{\mathrm{eff}}(\mathbf{k}', z_1, z_2)^{\dagger}\mathbf{G}(\mathbf{k}', z_2) = \hat{\boldsymbol{\Gamma}}_{\gamma}(z_1, z_2)$$

and

$$\lambda_{L_3L_4}^{L_1L_2}(z_1, z_2) = \int_{\mathrm{BZ}} \frac{\mathrm{d}^3\mathbf{k}}{8\pi^3} G_{L_3L_4}(\mathbf{k}, z_1)G_{L_2L_1}(\mathbf{k}, z_2)$$

$$\omega_{L_3L_4}^{L_1L_2} = W_{L_3}^{L_1}\delta_{L_1L_2}\delta_{L_3L_4}$$

$$W_{L'}^{L} = F_L(z_2)\left[\delta_{LL'} + 2\sum_{L''}[B_{L''}(z_1)G_{RL'',RL'}(z_1) \cdots + B_{L''}(z_2)G_{RL'',RL'}(z_2)]\right]F_{L'}(z_1)$$

$$F_L(z) = \sqrt{xy}\,\delta\left(\frac{C_L - z}{\Delta_L}\right)\Big/\langle\!\langle 1/\Delta_L\rangle\!\rangle$$

$$B_L(z) = (y - x)\delta\left(\frac{C_L - z}{\Delta_L}\right)\Big/\langle\!\langle 1/\Delta_L\rangle\!\rangle.$$

Here x, y are the concentrations of the component atoms, C, Δ are the standard potential parameters of the TB-LMTO and $\delta(f) = f_A - f_B$. These super-matrices in $\{L\}$ space are written as $\underline{\underline{\lambda}}$ and $\underline{\underline{\omega}}$. The full ladder vertex may now be written as

$$\underline{\underline{\Lambda}}(z_1, z_2) = \underline{\underline{\omega}} + \underline{\underline{\omega}}\,\underline{\underline{\lambda}}\,\underline{\underline{\omega}} + \underline{\underline{\omega}}\,\underline{\underline{\lambda}}\,\underline{\underline{\omega}}\,\underline{\underline{\lambda}}\,\underline{\underline{\omega}} + \cdots = \underline{\underline{\omega}}(\underline{\underline{I}} - \underline{\underline{\lambda}}(z_1, z_2)\underline{\underline{\omega}})^{-1}. \tag{9}$$

The averaged correlation function is then

$$\langle\!\langle S_{\gamma}(z_1, z_2)\rangle\!\rangle = \langle\!\langle S_{\gamma}^{(1)}(z_1, z_2)\rangle\!\rangle + \langle\!\langle S_{\gamma}^{(2)}(z_1, z_2)\rangle\!\rangle + \langle\!\langle S_{\gamma}^{\mathrm{ladder}}(z_1, z_2)\rangle\!\rangle. \tag{10}$$

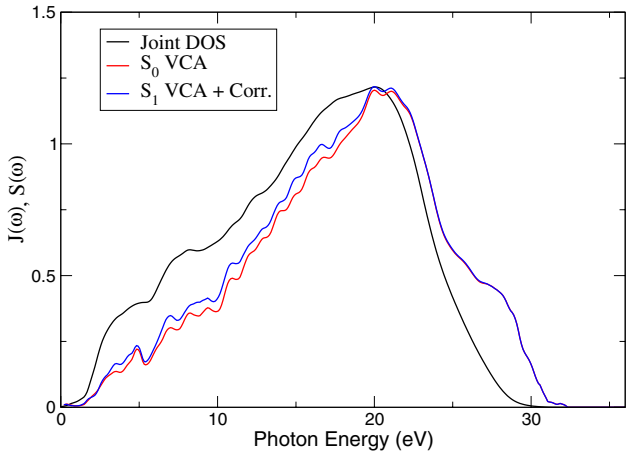

Figure 1. The configuration averaged joint density of states and correlation function for CuAu (50–50) alloy shown as a function of the photon energy.

Table 1. Lowest energy and Vegard's law lattice constants for CuAu and NiPt.

Alloy	Lowest energy lattice const (A)	Vegard's law lattice const (A)
$Cu_{50}Au_{50}$	7.31	7.26
$Ni_{50}Pt_{50}$	7.09	7.03

2. Results and discussion

We have begun our study with the self-consistent TB-LMTO-ASR calculation on NiPt and CuAu 50–50 alloys. We have minimized the energy with respect to the variation in the average lattice constant for both the alloys. Table 1 shows the lowest energy lattice constants and compares them with the averaged or Vegard law results. As expected, because of the large size difference between the constituents there is a 'bowing' effect, which is most prominent for the 50–50 alloys. The lowest energy lattice constant for both the alloys is greater than the Vegard law predictions.

Figure 1 shows the comparison between the scaled joint density of states and the averaged correlation function for a CuAu (50–50) alloy. From the figure it is clear that the transition rate is dependent both on the initial and the final energies, throughout the frequency range of interest. That is,

$$S(\omega) \neq |T|^2 J(\omega)$$

where

$$J(\omega) = \int \mathrm{d}E \int \frac{\mathrm{d}^3\mathbf{k}}{8\pi^3} \mathrm{Tr}\langle G^c(\mathbf{k}, E) G^v(\mathbf{k}, E+\omega)\rangle.$$

Figure 1 also shows that the disorder corrections to the current and the vertex correction are rather small and become negligible beyond photon energies of the order of 22 eV.

Figure 2 shows the optical conductivity for CuAu (50–50) alloy. The inset shows the configuration averaged density of states for the same alloy. The edge of the d-band complex is clearly seen to lie about 1 eV below the Fermi energy. The optical conductivity rapidly

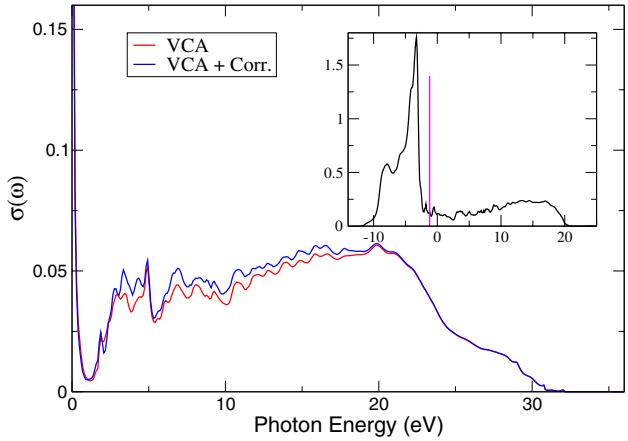

Figure 2. Averaged optical conductivity and the density of states for a CuAu (50–50) alloy, with the Fermi energy marked on it.

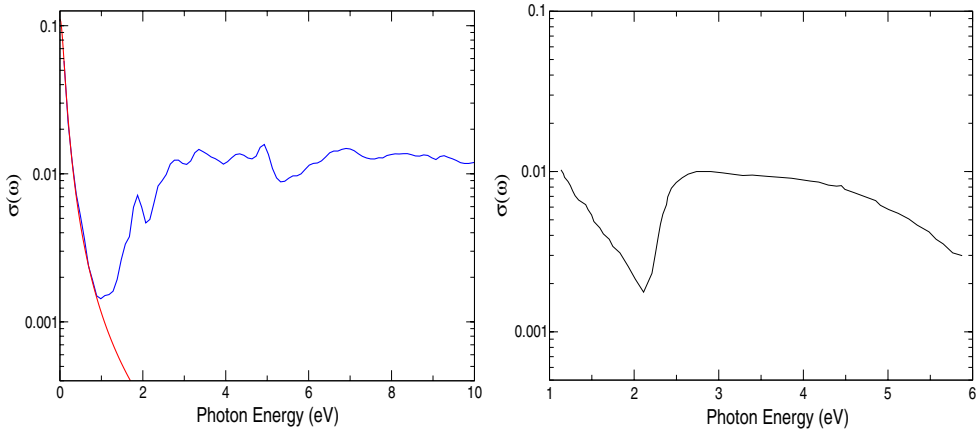

Figure 3. Left: averaged optical conductivity showing a Drude fit at low photon energies. Right: experimental data of $\sigma(\omega)$ in disordered CuAu taken from Scott and Muldawer [7].

decreases as we increase the photon energy from zero upwards. This decrease continues until about 1 eV and then the conductivity rises again and has considerable structure as also shown in the correlation function for these photon energies (figure 1).

Figure 3 (left) shows the optical conductivity with a Drude fit for the lower photon energies. The Drude fit is good for photon energies below 1.5 eV. From this information we may deduce that for low photon energies the conductivity arises due to intra-band transition between the s–p states, which are free-electron-like and lead to a Drude type behaviour. Above 1.5 eV there is a onset of inter-band transition between the d and the conduction states, and this leads to a sharp increase of optical conductivity and structure reflecting the structures in the d-like states.

Experimental data on disordered CuAu (50–50) are available [7]. The authors have reported high resolution optical data for both ordered and disordered CuAu for photon energies between 1.2 and 6.2 eV. In figure 3 right, we show the experimental data for $\sigma(\omega)$ and compare it with the theoretical data in figure 3 (left). Drude-like behaviour is clearly seen till photon

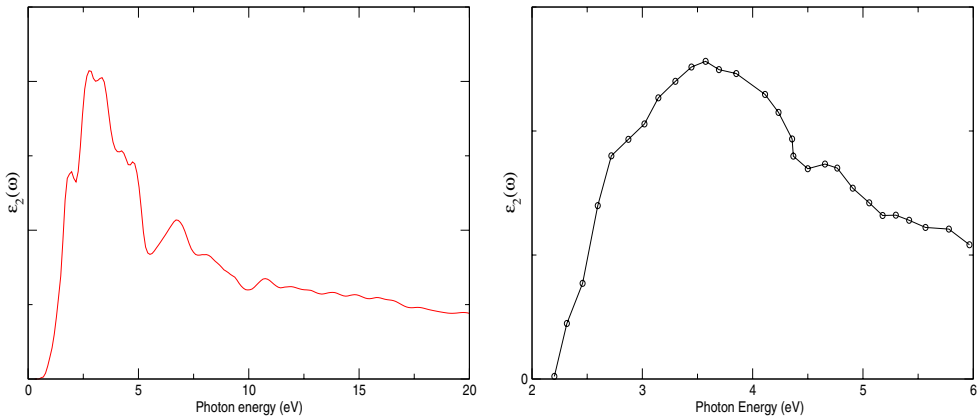

Figure 4. Intraband contribution to $\epsilon_2(\omega)$ for AgAu alloy. Left, theoretical; right, experimental (Banhart [8]).

energies of ∼1.6 eV in theory and around 2 eV in the experiment. Subsequently $\sigma(\omega)$ rises again because of transitions from the d states. Both the theory and experiment show a decrease around 6 eV. The comparison between the two is satisfactory.

We have experimental data on AgAu (50–50) [11], whose density of states closely resembles CuAu. The inter-band contribution to the imaginary part of the dielectric function $\epsilon_2(\omega)$ may be obtained from the optical conductivity data, by subtracting away the Drude contribution and dividing the result by ω: $\epsilon_2(\omega) = (\sigma(\omega) - \sigma^{\mathrm{D}}(\omega))/\omega$. Below the onset of the inter-band transitions, this quantity vanishes. It then reaches a maximum at around 3 eV before decreasing.

We have experimental data on AgAu (50–50) [11], whose density of states closely resembles CuAu. The experimental data are in good qualitative agreement with figure 4 (right). The general shape with a shoulder around 2 eV and a maximum just above 3 eV is clearly reproduced. However, as in Banhart's discussion, the discrepancy of a lateral shift of about 1 eV is also seen in our results as compared with experiment. This cannot be explained by the differences between CuAu and AgAu.

Figure 5 shows the joint density of states and the averaged correlation function for the NiPt (50–50) alloy. The energy–frequency dependence of the effective transition rate is considerable more pronounced than for CuAu. Disorder corrections to the current terms and vertex corrections are also greater in the low photon energy region. They become negligible for high photon energies.

Figure 6 (left) shows the density of states and the averaged optical conductivity for NiPt. Although the density of states for NiPt qualitatively resembles that for CuAu, unlike the latter the Fermi level sits right atop the high peak due to the d-like states. The inter-band transitions between the d states and the conduction band are expected to start for very small photon energies, with a Drude contribution confined to a very narrow energy range near zero. The optical conductivity falls sharply in a very narrow energy range and recovers almost immediately. This is expected from the density of states picture. Since the Drude fit is in a very narrow range indeed we do not show it explicitly in the figure.

As we were unable to locate experiments on the optical conductivity of NiPt, we turned to another alloy Nb_3Sb whose band structure resembles NiPt in the sense that the Fermi energy lies almost on a d-like peak. In figure 6 right, we show the optical conductivity of Nb_3Sb as reported by Gunnarsson *et al* [9]. We note the immediate similarity, with Drude behaviour

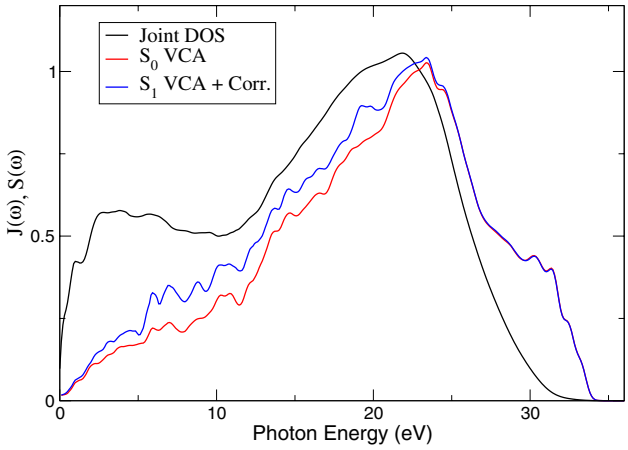

Figure 5. The configuration-averaged joint density of states and correlation function for NiPt (50–50) alloy shown as a function of photon energy.

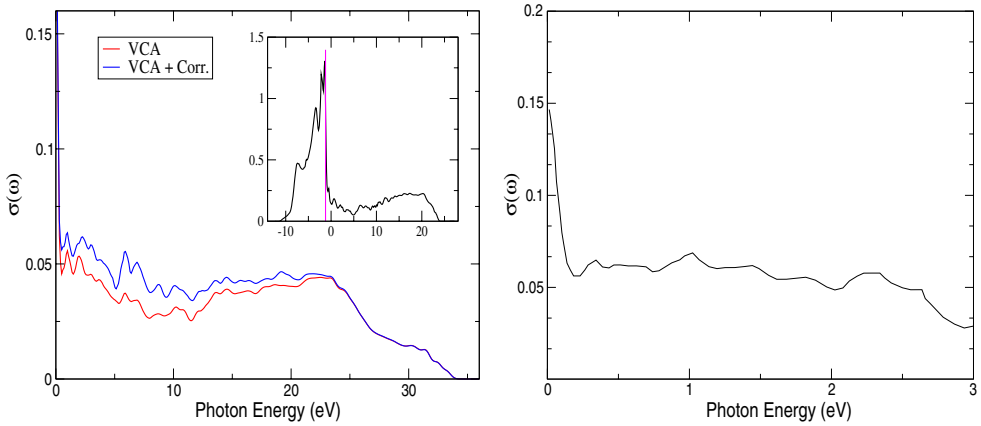

Figure 6. Left: averaged optical conductivity and the density of states for NiPt (50–50) alloy, with the Fermi energy marked on it. Right: the optical conductivity of Nb_3Sb as reported in [9].

in a very narrow range of photon energies and optical conductivity picking up very fast as transitions take place between the occupied d states and the unoccupied sp-like conduction states.

References

[1] Saha K K and Mookerjee A 2004 *Phys. Rev.* B **70** 134205
[2] Velický B 1963 *Phys. Rev.* **184** 614
[3] Butler W H 1985 *Phys. Rev.* B **31** 3260
[4] Gyorffy B L and Stott M J 1972 *Band Structure Spectroscopy of Metals and Alloys* ed D J Fabian and L M Watson (London: Academic)
[5] Gyorffy B L and Stocks G M 1978 *Electrons in Disordered Metals and at Metallic Surfaces* ed P Phariseau, B L Gyorffy and L Scheire (New York: Plenum)
[6] Sticks G M and Winter H 1984 *Electronic Structure of Complex Systems* (*NATO AST Series, Physics* vol B113) ed P Phariseau and W M Temmerman (New York: Plenum)

[7] Scott W R and Muldawer L 1976 *Phys. Rev.* B **14** 4426
[8] Banhart J 1999 *Phys. Rev. Lett.* **82** 2139
[9] Gunnarsson O, Calandra M and Han J E 2003 *Rev. Mod. Phys.* **75** 1085
[10] Rivory J 1977 *Phys. Rev.* B **15** 3119
[11] Nielsson P O 1970 *Phys. Kondens. Matter* **11** 1
[12] Saha T, Dasgupta I and Mookerjee A 1996 *J. Phys.: Condens. Matter* **8** 1979
[13] Mookerjee A 2003 *Electronic Structure of Alloys, Surfaces and Clusters* ed A Mookerjee and D D Sarma (London: Taylor and Francis) and the references therein
[14] Saha T and Mookerjee A 1996 *J. Phys.: Condens. Matter* **8** 2915
[15] Rhee J Y, Kudryavtsev Y V, Kim K W and Lee Y P 2000 *J. Appl. Phys.* **87** 5887
[16] Uba L, Uba S, Antonov V N, Yarenko A N and Gontarz R 2001 *Phys. Rev.* B **64** 125105
[17] Rhee J Y, Kudryavtsev Y V and Lee Y P 2003 *Phys. Rev.* B **68** 045104
[18] Andersen O K 1975 *Phys. Rev.* B **12** 3060
[19] Jepsen O and Andersen O K 1971 *Solid State Commun.* **9** 1763
[20] Mookerjee A 1973 *J. Phys. C: Solid State Phys.* **6** 1340
[21] Ghosh S, Das N and Mookerjee A 1999 *Int. J. Mod. Phys.* B **21** 723
[22] Kaplan T and Gray L J 1977 *Phys. Rev.* B **15** 3260